



MIXED CONVECTION PHENOMINA AFFECTED BY RADIATION IN A HORIZONTAL RECTANGULAR DUCT WITH COCENTRIC AND ECCENTRIC CIRCULAR CORE

Manal H. AL-Hafidh

Raed Gatie Sayhood

Ass. Prof. /University of Baghdad

Mechanical Engineer

ABSTRACT

The numerical investigation has been performed to study the radiation affected steady state laminar mixed convection induced by a hot inner varied positions circular core in a horizontal rectangular channel for a fully developed flow. To examine the effects of thermal radiation on thermo fluid dynamics behavior in the eccentric geometry channel, the generalized body fitted co-ordinate system is introduced while the finite difference method is used for solving the radiative transport equation. The governing equations which used are continuity, momentum and energy equations. These equations are normalized and solved using the Vorticity-Stream function. After validating numerical results for the case without radiation, the detailed radiation effect is discussed. From the parametric study, the Nusselt number (Nu) distributions in steady state were obtained for Aspect Ratio AR (0.55-1) and Geometry Ratio GR (0.1-0.9). The fluid Prandtl number is 0.7, Rayleigh number ($0 \leq Ra \leq 10^4$), Reynolds number Re (1-2000), Optical Thickness ($0 \leq t \leq 10$), Conduction-Radiation parameter ($0 \leq N \leq 100$) for the range of parameters considered. It is indicated in the results that heat transfer from the surface of the circular core exceeds that of the rectangle duct and when circular core is lower than the center of the channel, the rate of heat transfer decreased. The correlation equations are concluded to describe the radiation effect.

:

()
-
(0.1-0.9)
Re (1- (0 ≤ Ra ≤ 10⁴) (Pr = 0.7) (0.55-1)
(0 ≤ N ≤ 100) - (0 ≤ t ≤ 10) 1000)

KEY WORDS: mixed convection, radiation, rectangular duct, circular core, laminar flow.

INTRODUCTION:

Fully developed mixed convection laminar flow phenomena occur in a wide range of engineering applications as heat exchangers, solar collector, electronic equipment and similar devices. For this purpose various investigations have been performed in the literature under different boundary and operating conditions in order to maximize the heat transfer under optimum channel geometries.

Initial investigations on the heat transfer in channels neglected natural convection effects and only studied forced convection. In low Reynolds number flow conditions, both heat transfer mechanisms play a vital role and both have to be accounted for in which the heat transfer is being considered as mixed convection. [Pu et al, 1991] reported experimental results of mixed convection heat transfer in a vertical packed channel with asymmetric heating of opposing walls. The experiments were carried in the range of ($2 < Pe < 2200$) and ($700 < Ra < 1500$). The measured temperature distribution indicates the existence of secondary convection cell inside the vertical packed channel in the mixed convection regime.

Transfer of heat by simultaneous convective and radiative transfer at high temperature and high heat fluxes has become increasingly important in the analysis and design of high temperature gas – cooled nuclear reactors, advanced energy conversion devices, furnaces, combustors etc. these and many other applications have provided the impetus for research on combined convection radiation in participating media. [Larson and Viskanta, 1976] studied the transient laminar free convection and radiation in a rectangular enclosure. The effects of non participating radiation, wall heat conduction and laminar natural convection were examined. The results indicate that radiation dominates the heat transfer in the

enclosure and alters the convective flow patterns significantly.

[Kim and Viskanta, 1984] studied the effects of wall conduction and radiation heat exchanger among surfaces on laminar free convection heat transfer in a two – dimensional rectangular cavity modeling a cellular structure. The local and average Nusselt numbers were reported along the cavity walls for a range of physical interest. The local heat transfer rate was found to depend not only on the natural convection in the cavity but also on the wall conductance and radiation parameters. The results indicate that natural convection heat transfer in the cavity is reduced by heat conduction in the walls and radiation exchanger among surfaces.

[Bahlaoui, Raji, and Hasnoui, 2005] studied numerically a mixed convection coupled with radiation in an inclined channel with constant aspect ratio and locally heated from one side. The convective radiative and total Nusselt numbers were evaluated on the cold surface and at the exit of the channel and for different combinations of the governing parameters. The results obtained show that the flow structure is significantly altered by radiation which contributes to reduce or to enhance the number of the solutions obtained.

[Gururaja Rao, 2004] reported the results of an exhaustive numerical investigation into the problem of multi – mode heat transfer from a vertical channel for the twin cases of (i) uniform and (ii) discrete wall heat generation. Two –dimensional, steady state, incompressible, conjugate, laminar mixed convection with surface radiation is considered in both cases. The effects of parameters, such as surface emissivity, aspect ratio, modified Richardson number and discrete heat source position on the fluid flow and heat transfer characteristics are clearly brought out.

In the present investigation, the fully developed laminar mixed convective and radiative heat transfer will be investigated in an horizontal rectangular channel with interior circular core. The channel is fixed and the effect of heat generation is studied for thermal boundary condition of constant wall temperature and for $(0.1 \leq GR \leq 0.9)$, $(0.55 \leq AR \leq 1)$, $(1 \leq Re \leq 2000)$, $(0 \leq Ra \leq 10^4)$, $(0 \leq N \leq 100)$

MATHEMATICAL MODEL

Consider the steady state flow in an annulus of a rectangular channel with varied positions circular core as shown in **Fig. (1)**. This annulus is symmetrical about Y-axis ($\partial/\partial x = 0$). The flow is hydro dynamically and thermally fully developed laminar flow. The working fluid is assumed absorbing, emitting and the fluid properties are assumed constant except for density variation with temperature resulting in the secondary flows generated by the buoyancy forces. The axial (z) direction shown in **Fig. (1)** is the predominant direction for the fluid flow. The flow is laminar, and viscous dissipation effects are neglected. Axial conduction and radiation are assumed negligible following [Yang and Ebdian, 1991].

Governing Equations:

Assuming two – dimensional flow with constant properties, the governing equations for the vorticity – stream function and the temperature at steady state conditions are:

Stream Function Equation

$$-\omega = \frac{\partial^2 \psi}{\partial X^2} + \frac{\partial^2 \psi}{\partial Y^2} \tag{1}$$

Axial Momentum Equation

$$\frac{\partial \psi}{\partial Y} \frac{\partial W}{\partial X} - \frac{\partial \psi}{\partial X} \frac{\partial W}{\partial Y} = \left(\frac{\partial^2 W}{\partial X^2} + \frac{\partial^2 W}{\partial Y^2} \right) + 4 Re \frac{Ra \sin \lambda}{Pr} (1 - \theta) \tag{2}$$

Dimensionless Energy Equation

$$\frac{\partial \psi}{\partial Y} \frac{\partial \theta}{\partial X} - \frac{\partial \psi}{\partial X} \frac{\partial \theta}{\partial Y} = \frac{1}{Pr} \left(\frac{\partial^2 \theta}{\partial X^2} + \frac{\partial^2 \theta}{\partial Y^2} \right) - \frac{W}{Pr} + \frac{N t^2}{4 Pr} (1 - \theta^4) \tag{3}$$

Where the stream function ψ is defined in terms of the axial and radial velocities as follows respectively:

$$U = \frac{\partial \psi}{\partial Y}, \quad V = -\frac{\partial \psi}{\partial X} \tag{4}$$

The last term of eq. (3) represents the radiation absorption term.

Normalization Parameters

The variables in the governing equations and boundary conditions were transformed to dimensionless formula by employing the following transformation parameters:

$$X = \frac{x}{d}, \quad Y = \frac{y}{d}, \quad Z = \frac{z}{d}$$

$$U = \frac{ud}{\nu}, \quad V = \frac{vd}{\nu}, \quad W = \frac{wd}{\nu}$$

$$\theta = \frac{T}{T_w}, \quad \frac{\partial p}{\partial z} = -\frac{4\rho\nu^2}{d^3} Re, \quad \frac{\partial T}{\partial z} = \frac{T_w}{Pr d},$$

$$Pr = \frac{\nu}{\alpha}$$

$$N = \frac{4\sigma \epsilon T_w^3}{K_R k}, \quad t = K_R d, \quad U = \frac{\partial \psi}{\partial Y},$$

$$V = -\frac{\partial \psi}{\partial X}$$

The boundary conditions applicable to these equations are:

(1) At the inlet of the duct ($Z = 0$):

$$U = V = \psi = \omega = 0, \quad \theta = 0.5, \quad W = \frac{Re}{\nu d}$$

(2) At the walls:

$$U = V = W = \psi = 0, \quad \theta = 1$$

$$\frac{\partial \theta}{\partial X} = \frac{\partial \psi}{\partial X} = \frac{\partial \omega}{\partial X} = \frac{\partial W}{\partial X} = 0 \quad (\text{at symmetry line})$$

NUMERICAL METHODS

The elliptic transformation technique which was originally proposed by [Fletcher, 1988] is applied to generate the curvilinear grid for dealing with the irregular cross sections. The transformation functions $\xi = \xi(X, Y)$ and $\eta = \eta(X, Y)$ are obtained to accommodate the irregular shape. Using the curvilinear grid obtained the governing eq. (1) to (3) and the boundary conditions are then discretized and solved in the computation domain (ξ, η) . In this work, an (81 X 61) grid in the transformed domain (ξ, η) is adopted. The grid systems have been properly adjusted to be orthogonal locally at the boundaries. The grid generation technique used is standard and well accepted. Therefore, further description about this technique would not give here.

By using this method, the following general equation can be used to generate all the governing equations (1-3) in computational coordinate's formula:

$$J\Gamma(\psi_{\eta}\phi_{\xi} - \psi_{\xi}\phi_{\eta}) = (\tau\phi_{\xi} + \varpi\phi_{\eta} + \alpha_1\phi_{\xi\xi} - 2\beta_1\phi_{\xi\eta} + \gamma\phi_{\eta\eta}) + suJ^2 \quad (5)$$

Where Φ represent the general variable which may be ω , W or θ and su is the source term. Where $\Gamma = 1$ for vorticity transport and axial momentum equations and $\Gamma = Pr$ for energy equation.

Finite Difference Formulation:

The three-point central difference formula is applied to all the derivatives. Each of

the governing equations can be rewritten in a general form as:

$$ap_{(i,j)}\phi_{(i,j)} = ae_{(i,j)}\phi_{(i+1,j)} + aw_{(i,j)}\phi_{(i-1,j)} + an_{(i,j)}\phi_{(i,j+1)} + as_{(i,j)}\phi_{(i,j-1)} + SU_{(I,J)}J_{(I,J)} \quad (6)$$

Where:

$$ap_{(i,j)} = 2(\alpha_{1(i,j)} + \gamma_{(i,j)})$$

$$ae_{(i,j)} = \alpha_{1(i,j)} - B$$

$$aw_{(i,j)} = \alpha_{1(i,j)} + B$$

$$an_{(i,j)} = \gamma_{(i,j)} - C$$

$$as_{(i,j)} = \gamma_{(i,j)} + C$$

$$B = \left(J_{(i,j)}\Gamma \frac{\psi_{(i+1,j)} - \psi_{(i-1,j)}}{2} - \tau_{(i,j)} \right) / 2$$

$$C = \left(-J_{(i,j)}\Gamma \frac{\psi_{(i,j+1)} - \psi_{(i,j-1)}}{2} - \varpi_{(i,j)} \right) / 2$$

$$SU_{(I,J)} =$$

$$- \frac{\beta_{1(i,j)}}{2J_{(i,j)}} (\phi_{(i+1,j+1)} - \phi_{(i+1,j-1)} - \phi_{(i-1,j+1)} + \phi_{(i-1,j-1)})$$

$$+ su_{(i,j)}J_{(i,j)}$$

In the equations above i and j indicate to the points of the grid in the generalized coordinates ξ and η respectively.

As pointed out in [Anderson et al, 1984] the Relaxation method can be employed for the numerical solution of eq. (1). For this investigation, the Line Successive Over Relaxation (LSOR) method [Fletcher, 1988] and [Anderson et al, 1984] is used to solve equations (2 and 3). A computer program (Fortran 90) is built to calculate Nu . The convergence criterion for the inner iteration ($Error_{in}$) of ψ is 10^{-4} and for the outer iteration ($Error_{out}$) of θ is 10^{-10} , where:

$$Error_{in} = 2(\alpha_{1(i,j)} + \gamma_{(i,j)})\Delta\psi_{(i,j)} \quad (7)$$

$$\Delta\psi_{(i,j)} = \frac{\psi_{(i,j)}^{it+1} - \psi_{(i,j)}^{it}}{RP} \quad (8)$$

Where RP is the Relaxation Parameter and equal 1.1 and represent the number of iterations. The outer iteration is checked only for θ_b as follow:

$$Error_{out} = \frac{\theta_b^{it+1} - \theta_b^{it}}{\theta_b^{it}} \leq 10^{-10} \quad (9)$$

EVALUATION OF HEAT TRANSFER:

The peripheral heat transfer is defined through the conduction referenced Nusselt number as:

Local Nusselt number

The peripheral local Nusselt number on the walls of the channel is computed from:

$$Nu_L = \frac{-\frac{\partial\theta}{\partial n}\Big|_w}{(1-\theta_b)} \quad (10)$$

Where n represent the dimensionless normal outward direction.

The mean Nusselt number on the wall of the rectangular duct and circular core is obtained by using Simpson's rule:

$$Nu_{c,r} = \frac{1}{s} \int_s Nu_L ds \quad (11)$$

Where s is represents the length of the wetted perimeter in the rectangular duct and circular core.

The mean Nusselt number (Nu) is a measure of the average heat transfer over the internal surface of the rectangular duct and the outer surface of the circular configuration. It is computed from the following equation:

$$Nu = C_c Nu_c + C_r Nu_r \quad (12)$$

Where, $C_c Nu_c$ is a measure of average heat transfer from the outer surface of the circular core while $C_r Nu_r$ corresponds to heat transfer from of the internal surface of the rectangular duct. C_c and C_r are the perimetric ratios for the heat transfer and are defined as:

$$C_c = \frac{\pi R}{H + L + \pi R}$$

$$C_r = \frac{H + L}{H + L + \pi R}$$

RESULTS AND DISSCUSION:

Effect of Circular Core Position:

The heat transfer process through the channel suffers from many changes in the heat transfer process because of the layer of the still air in the corners as shown in **Fig. (2)**. This layer cause to increase the thermal resistance and that lead to decrease the rate of heat transfer. The heat transfer rate through the wall of the circular core is uniform and greater than that on the walls of the rectangular duct. The direction of the heat transfer from the walls towards the core of the channel is shown by the isotherm lines.

The effect of the circular core position on the isotherms and streamlines for air is shown in **Fig. (2-6)**. It is shown when the circular core is lower than the center of the channel, the volume and intensity of the upper cell will be increased, while, for the lower cell its volume and intensity will be decreased until it is vanished because of increasing the cross section area above the circular core. But the lower area is decreased when the circular core is get down. This decreasing in the volume and intensity of the cells under the circular core will be lead to decrease the rate of heat transfer then decrease Nu as shown in **Fig (7)**.

Effect of GR:

. The bulk temperature of air increased with increasing in geometry ratio value as shown in **Fig. (8)** and that because of increasing in the surface area which participating in the heat transfer process

and that result to increase the rate of heat transfer.

Fig. (9) illustrates the variation of mean Nusselt number Nu through the channel with GR value. It is shown that when GR increased Nu increased and that resulting from increasing in the surface area of the circular wall. This increasing of the surface area will lead to increase the rate of heat transfer. The radiation effect is very small for the small values of GR . This effect increased with increasing in GR value because of increasing the heat gain by air with decreasing in the air quantity.

Fig (10) illustrates the change in the value of Nu_L along the wall of the circumference of the circular core with GR value. The value of Nu_L is approximately uniform and equally at small value of GR . For $GR > 0.4$, the value of Nu_L will be changed. and will be decreased in the throat regions because of impended of the wall to the vorticity and that lead to decrease the rate of heat transfer, while, in the other regions Nu_L will be increased because of increasing the intensity of vorticity and its center, and that results to increase the rate of heat transfer. But when GR reached 0.9, the value of Nu_L will be the maximum in the throat regions, this is resulted from the distance between the walls which is very small, and that lead to increase the rate of heat transfer.

Nu_{Lr} on the walls of the rectangular duct decreased with increasing in GR value in the throat regions as shown in **Fig (11)**, while, in the other regions the value of Nu_{Lr} increased when GR increased. The minimum value is approximately equal zero in the right corners of the rectangular duct, and that because of the decreasing in the rate of heat transfer resulting from increasing the thermal resistance of the semi-still air which is generated in these corners. The heat transfer rate through the wall of the circular core is uniform and greater than that on the walls of the rectangular duct.

Effect of Re:

Fig. (12-14) illustrate the isotherms and streamlines for different values of Re . These figures show that the increase in Re will not change the behavior of the stream function and the temperature distribution, but, it will be increase the intensity and the value of stream function and the temperature of the air.

The effect of Re on the value of Nu is shown in **Fig. (15)**, where it is shown that the value of Nu is decreased with increasing Re until it is reached the minimum value at $Re = 350$. But, Nu value will be something increased when Re is increased from 350. When $Re = 1$, the convection process is only natural convection, where the effect of the buoyancy force and the secondary flow had a vital role in the heat transfer process, and that lead to turn the streams of air widely through the cross section area of the channel. So, the increasing in Re is effected negatively on the heat transfer process, where it lead to increase the axial velocity of the flow and implement the vorticity of the air, but it is lower than the case of the natural convection. Also, the radiation effect is very small for the low values of Re , but its effect will be increased with increasing in Re value.

In **Fig. (16)** the effect of Ra on Nu value is shown with the variation in Re . This effect is approximately constant with the variation of Re value.

Radiation Effect:

The correlation equations for the plotted curves are done to know the radiation effect on the rate of heat transfer. These equations are made by using the curve fitting method.

$$Nu = 6.5677 + 39.176 GR^{2.887}$$

$$Nu = 13.0733 + 0.03231 AR^{-9.0938}$$

(Without radiation)

$$Nu = 7.577 + 44.648 GR^{3.1}$$

$$Nu = 12.117 + 0.58597 AR^{-4.55}$$

(With radiation)

For the bulk temperature, the effect of radiation will be written as follow:

$$\theta_b = -12.287 + 13.304 GR^{6.2 \times 10^{-3}}$$

(With Radiation)

$$\theta_b = -15.747 + 16.763 GR^{5.4 \times 10^{-3}}$$

(Without Radiation)

CONCLUSIOS:

- From the present work results and for the channel that described previously, the following conclusions can be obtained:
 - When the circular core is lower than the center of the channel, the volume and intensity of the upper cell will be increased, while, for the lower cell its volume and intensity will be decreased.
 - The decrease in the volume and intensity of the cells under the circular core lead to decrease the rate of heat transfer
 - The bulk temperature of air increased with increasing in geometry ratio. When GR increased Nu increased and that resulting from increasing in the surface area of the circular wall. The value of Nu_L is approximately uniform and constant at small value of GR. For $GR > 0.4$, the value of Nu_L will be changed, and will be decreased in the throat regions but when GR reached 0.9, the value of Nu_L will be the maximum in the throat regions. Nu_{Lr} on the walls of the rectangular duct decreased with increasing in GR value in the throat regions, while, in the other regions the value of Nu_{Lr} increased when GR increased. The minimum value is approximately equal zero in the right corners of the rectangular duct
- The increases in Re will not change the behavior of the stream function and the temperature distribution, but, it will be increase the intensity and the value of stream function and the temperature of the air.
 - Nu decrease by 33% with increasing in Re and at Ra = 400, while it is increased by 1% with increasing in Ra and at Re = 100.
 - The radiation effect is very small for the low values of Re, but its effect will be increased with increasing in Re value.
 - The radiation effect on the heat transfer coefficient is known by making a correlation equations and this effect show that Nu will be increased.

REFERENCES

- Anderson A., Tannehill C. and Pletcher H. (1984), "Computational Fluid Mechanics and Heat Transfer", McGr
- Bahlaoui A., Raji A., and Hasnoui M., (2005), "Multiple Steady State Solutions Resulting From Coupling Between Mixed Convection and Radiation In An Inclined Rectangular Channel", Int. J. of Mass Heat Transfer
- (<http://www.springerlink.com/content/rv03480249507w41/>).
- Fletcher C. A. J., (1988), "Computational Fluid Techniques for Fluid Dynamics 2", Springer-Verlag.
- Gururaja Rao C., (2004), "Numerical Investigation into Multi-Mode Heat Transfer from a Vertical Channel with Uniform and Discrete Wall Heat Generation", HPC 2004-3th International Conference on Heat Powered Cycles.
- Kim D. M. and Viskanta R., (1984), "Heat Transfer by Conduction, Natural Convection and Radiation across a Rectangular Cellular Structure", Int. J. of Heat and Fluid Flow, Vol.5, No.4, PP.205-213
- (www.springerlink.com/index/6R7T68Q705W73311.pdf).
- Larson D. W. and Viskanta R., (1976), "Transient Combined Laminar Free Convection and Radiation in a Rectangular Enclosure", J. Fluid Mechanics, Vol.78, Part 1, PP.65-85.
- Pu W. L., Cheng P. and Zho T. S., (1991), "An Experimental Study of Mixed Convection Heat Transfer in Vertical Packed Channel", AIAA, J. of Thermophysics and Heat Transfer, Vol.13, No.4, PP.517-521.
- Yang G. and Ebdian M. A., (1991), "Thermal Radiation and Laminar Forced Convection in the Entrance of a Pipe With Axial Conduction and Radiation", Int. J. Heat Fluid Flow, Vol.12, no. 3, pp. 202-209.

NOMENCLATURE

Symbol	Description	Units
AR	Aspect ratio ($AR = L/H$)	-
D	The diameter of circular core	m
d	The hydraulic diameter of the channel	m
H	The height of the rectangular duct	m



J	Jacobean of direct transformation	-
Symbol	Description	Units
k	Thermal conductivity of the air	W/m. °C
K_R	Volumetric absorption coefficient	m^{-1}
L	The width of the rectangular duct	m
N	Conduction-radiation parameter($4\sigma\epsilon T_w^3/K_R k$)	-
Nu	The mean Nusselt number	-
Nu_{LC}, Nu_{Lr}	The local Nusselt number in the circular and rectangular walls respectively	-
P_c, P_r	Wetted perimeter for the circular and rectangular walls respectively	m
Pr	Prandtl number ($Pr = \nu/\alpha$)	-
R	The circular core radius	m
Ra	Rayleigh number ($Ra = \beta g d^3 T_w / \alpha \nu$)	-
Re	Reynolds number [$Re = (-d^3/4\rho\nu)(\partial P/\partial z)$]	-
GR	Geometry ratio ($GR = D/H$)	-
T	Air temperature	°C
t	Optical thickness($t = K_R D_h$)	-
T_w	Wall temperature	°C
u, v, w	The velocity components in x, y and z direction respectively	m/s
U, V, W	The normalized velocity components in x, y and z direction respectively	-
x, y, z	The physical coordinates of the channel	m

X, Y, Z	The dimensionless physical coordinates of the channel	-
---------	---	---

GREEK SYMBOLS

Symbol	Description	Units
α	Thermal diffusivity	m ² /s
$\alpha_s, \beta_s, \gamma, \omega, \tau$	The coefficient of transformation of BFC	-
β	Coefficient of thermal expansion	1/K
ε	Emissivity	-
ξ, η	Coordinates in the transformed domain	m
θ	Dimensionless air temperature	-
θ_b	Dimensionless bulk temperature	-
θ_c, θ_r	Dimensionless temperature of the circular core and rectangular duct walls respectively	-
θ_w	Dimensionless wall temperature	-
ν	Kinematics' viscosity of air	m ² /s
ρ	Air density	kg/m ³
σ	Stefan Boltzmann constant	W/m ² K ⁴
ψ	Dimensionless air stream function	-
ω	Dimensionless air vorticity	-

SUPERSCRIPTS AND SUBSCRIPTS

Symbol	Description	Units
b	Bulk	-
C	Circular core	-
g	Generation	-
(i, j)	Grid nodes in X and Y directions	-
L	Local	-
<i>r</i>	<i>rectangular duct</i>	-
<i>w</i>	<i>Wall</i>	-
Symbol	Description	Units
°	<i>Degree</i>	-
-	<i>Average</i>	-

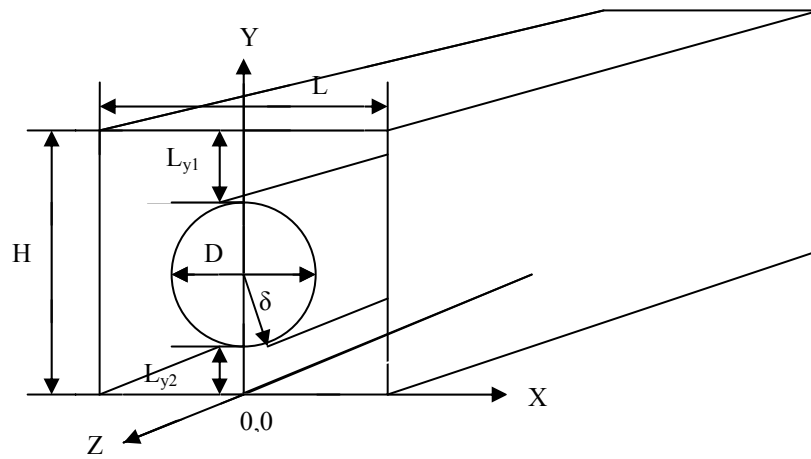


Fig.(1) Schematic of the Problem Geometry

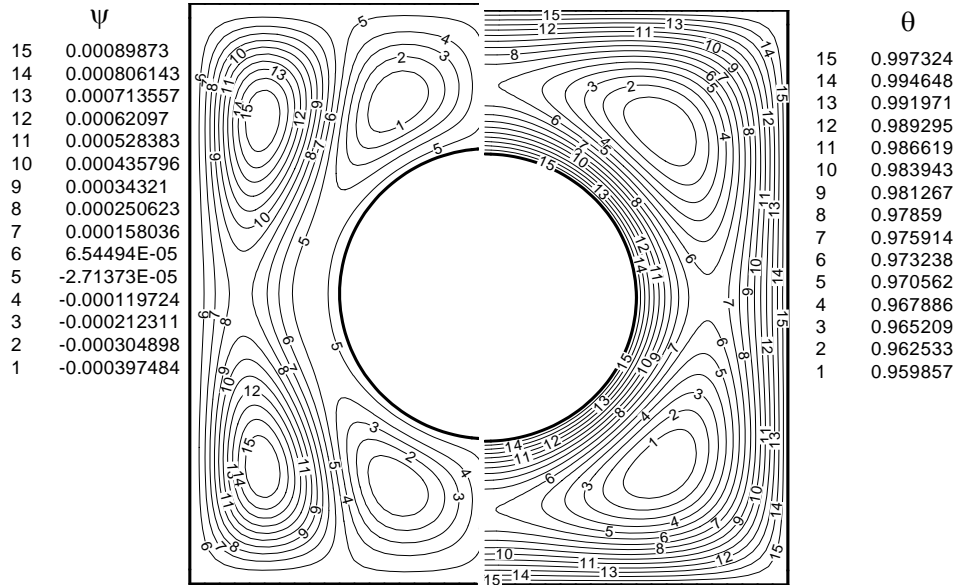


Fig. (2) Streamlines and Isotherms for Concentric Core and for $GR = 0.5$

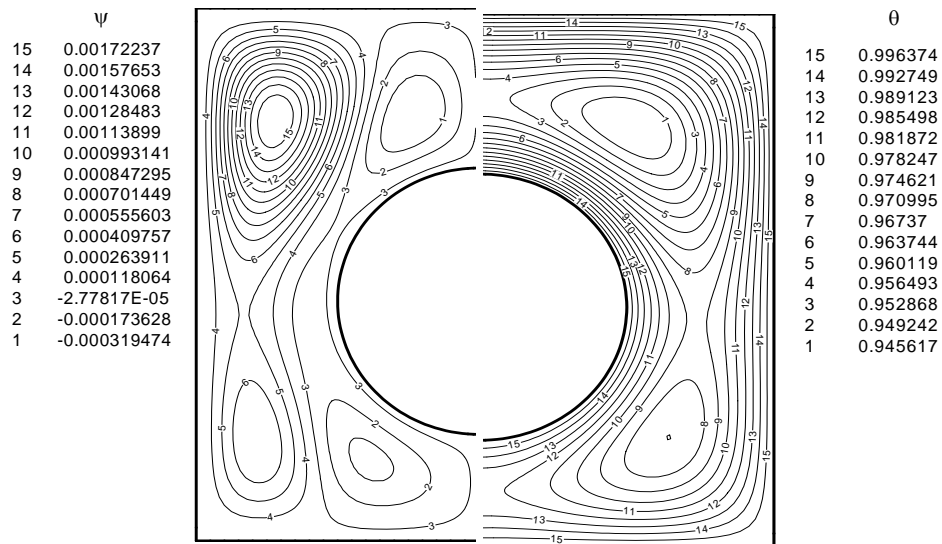


Fig. (3) Streamlines and Isotherms for $Ly_2 = 0.3$

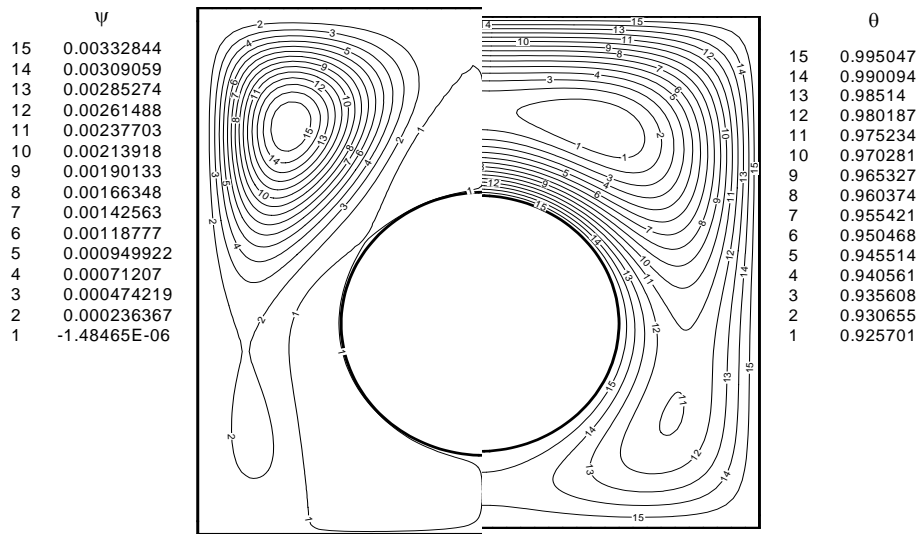


Fig. (4) Streamlines and Isotherms for $Ly_2 = 0.35$

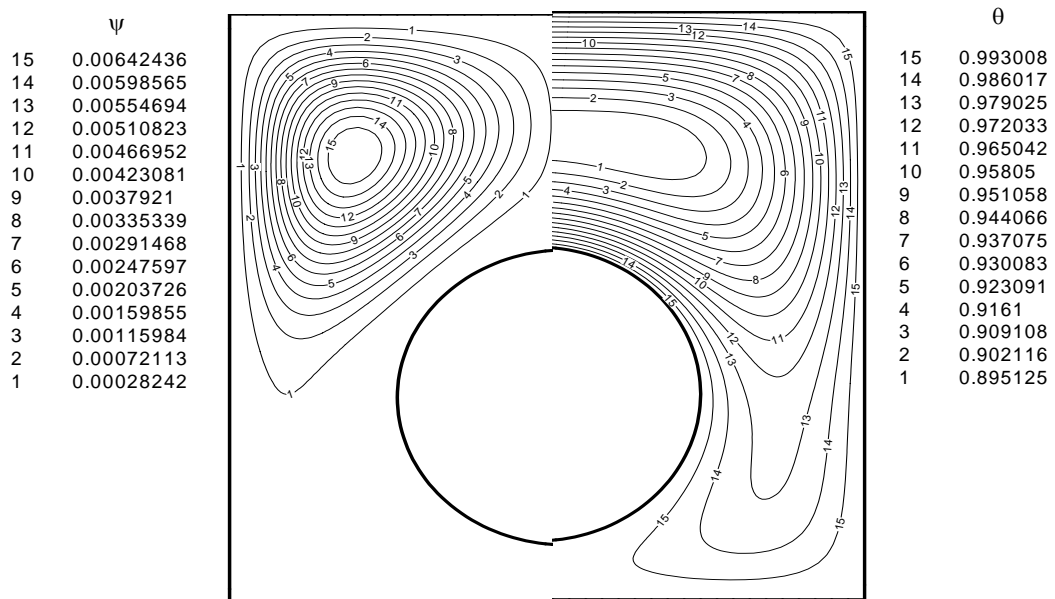


Fig. (5) Streamlines and Isotherms for $Ly_2 = 0.4$

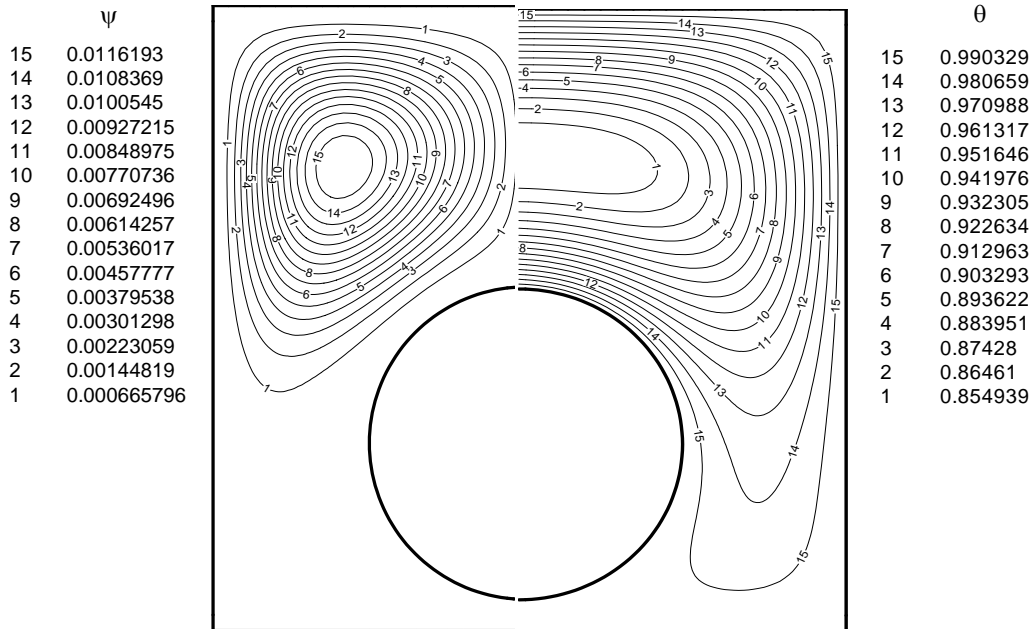


Fig. (6) Streamlines and Isotherms for $Ly_2=0.45$

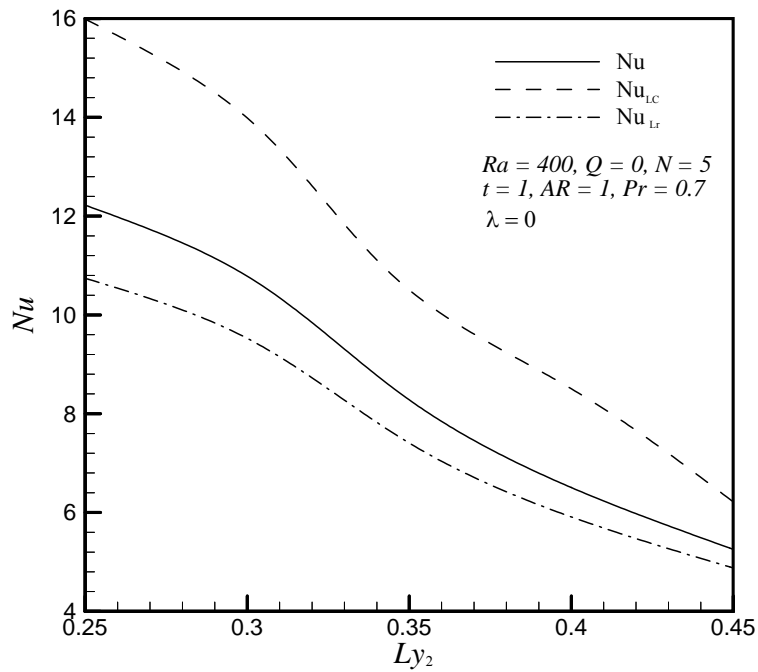


Fig. (7) The Effect of Circular Core Positions

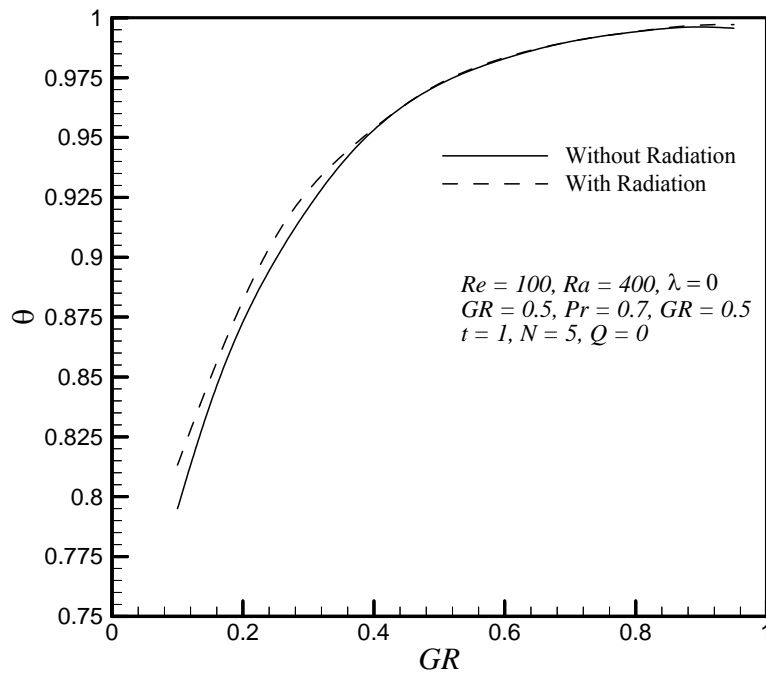


Fig. (8) The Effect of Geometry Ratio on the Bulk Temperature

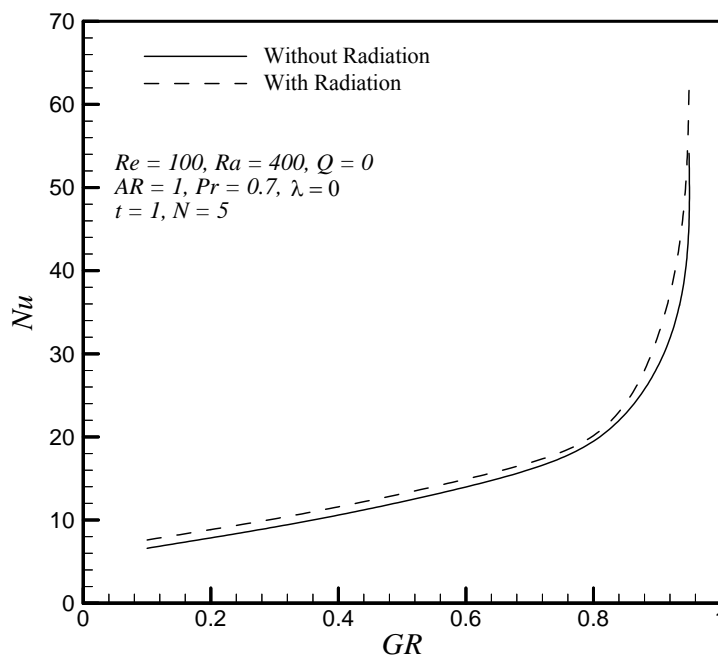


Fig. (9) The Variation of the Mean Nusselt Number with Geometry Ratio

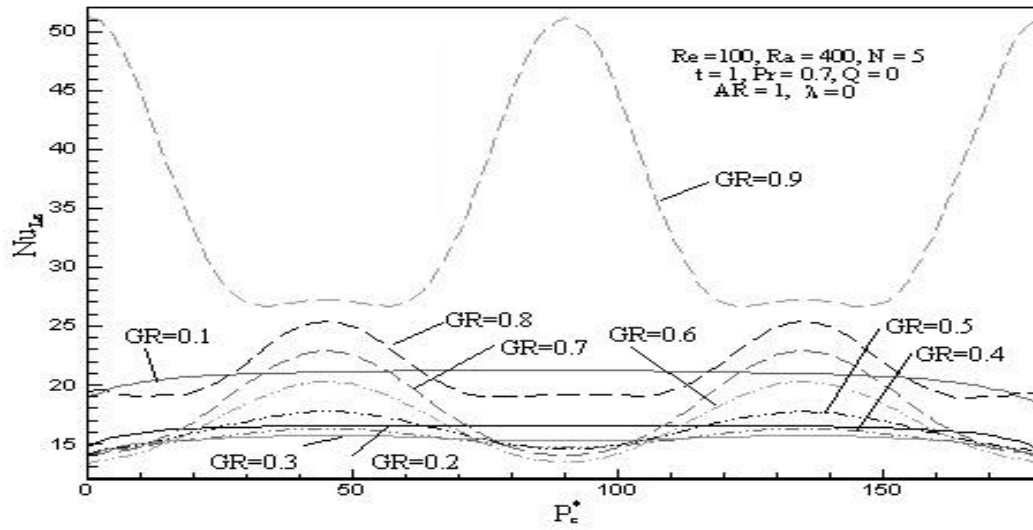


Fig. (10) The Variation of the Local Nusselt Number with P_c^*

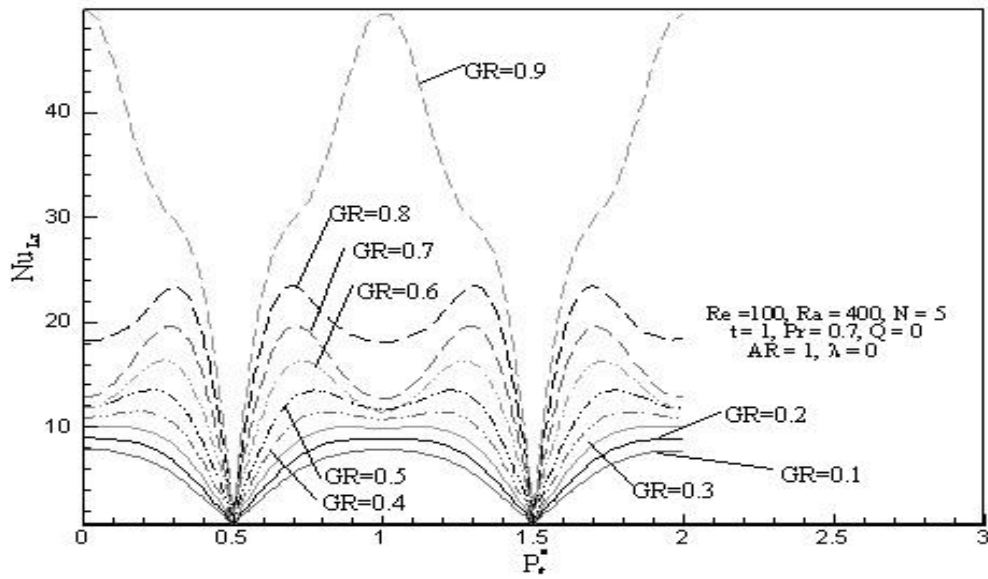


Fig. (11) The Variation of the Local Nusselt Number with P_r^*

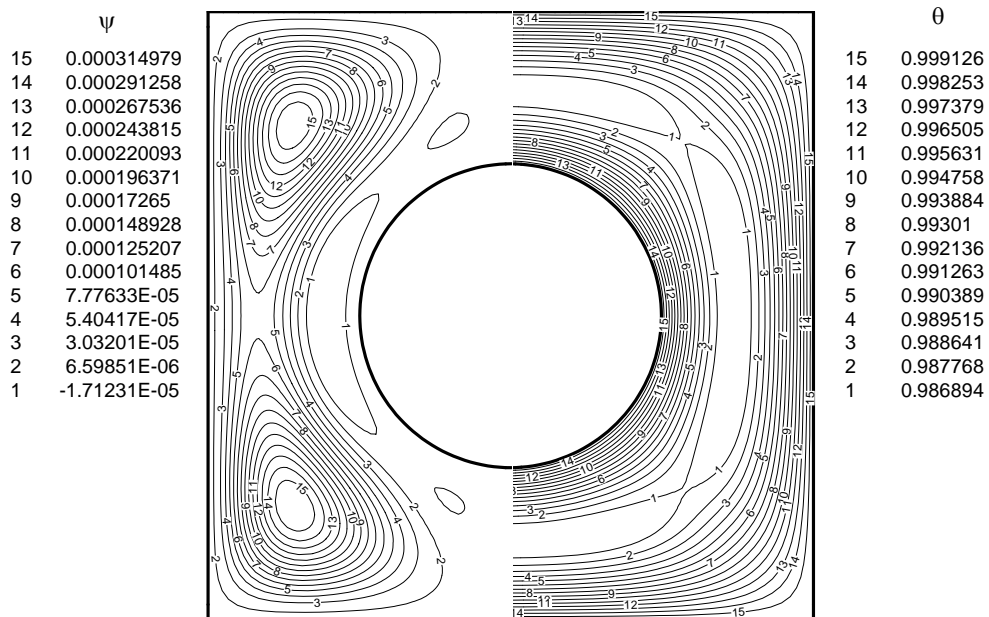


Fig. (12) Streamlines and Isotherms for $Re = 1$

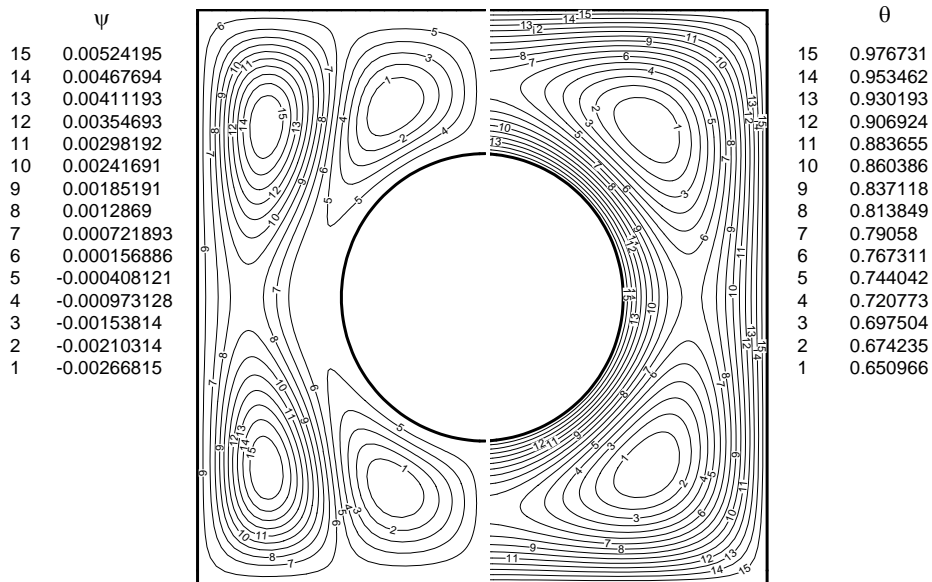


Fig. (13) Streamlines and Isotherms for $Re = 1000$

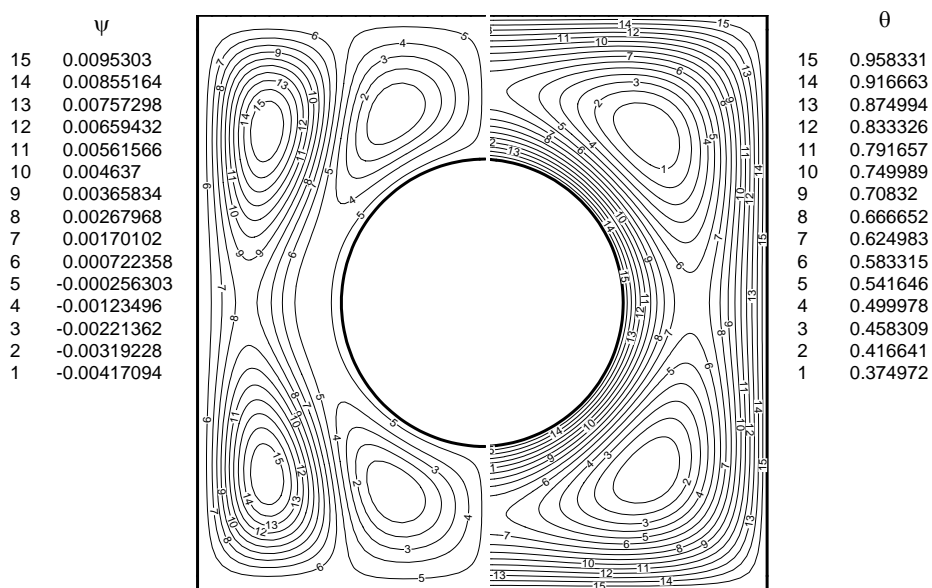


Fig. (14) Streamlines and Isotherms for $Re = 2000$

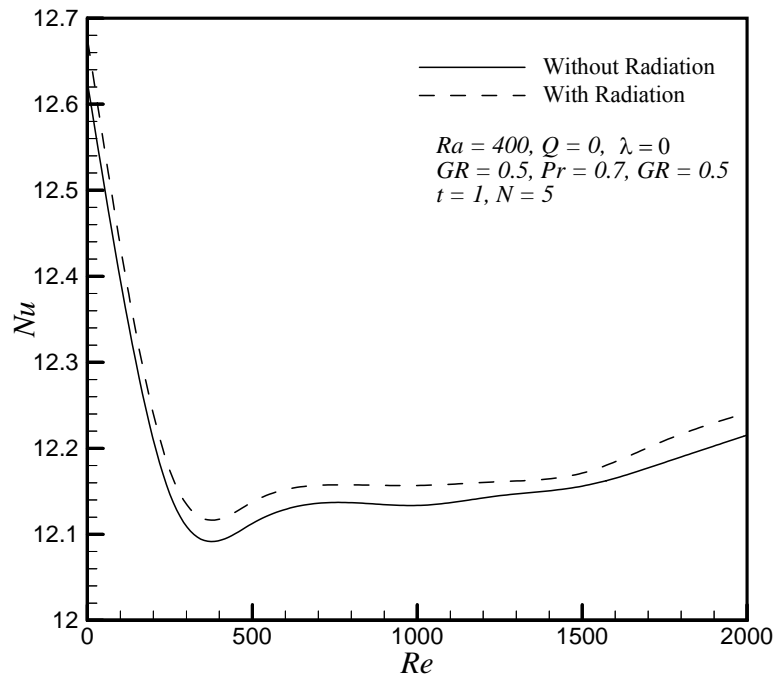


Fig. (15) The Variation of the Mean Nusselt Number with Reynolds Number

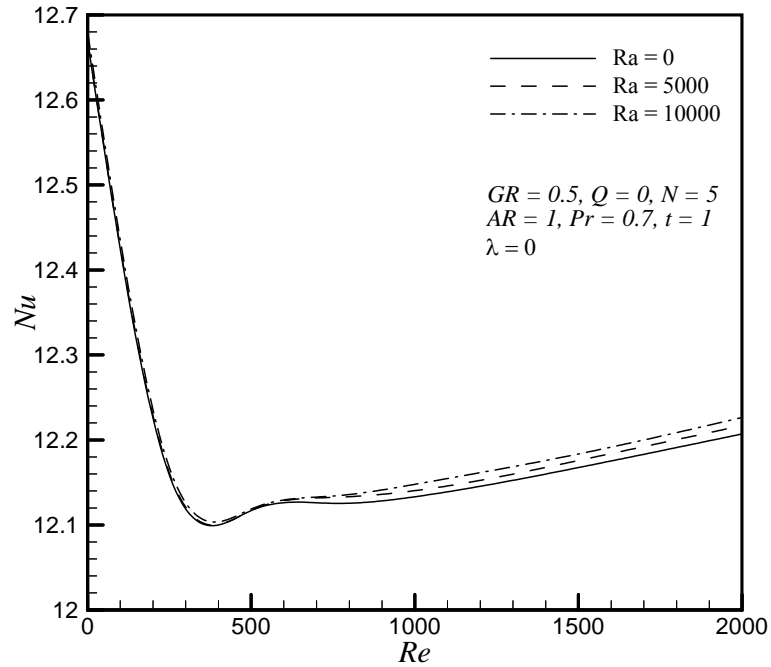


Fig. (16) The Variation of Nusselt Number with Re for Different Values of Ra